Comparison of apparent diffusion coefficients of resectable mid-high rectal adenocarcinoma and distal paracancerous tissue

HUI LUO[1], YUE-QIN GOU[1], YUE-SU WANG[1], HUI-LIN QIN[1], HAI-YING ZHOU[1], XIAO-MING ZHANG[1] and TIAN-WU CHEN[2]

[1]Medical Imaging Key Laboratory of Sichuan Province, Department of Radiology, Affiliated Hospital of North Sichuan Medical College, Nanchong, Sichuan 637000, P.R. China; [2]Department of Radiology, The Second Affiliated Hospital of Chongqing Medical University, Chongqing 400010, P.R. China

Received July 6, 2024; Accepted November 29, 2024

DOI: 10.3892/ol.2024.14843

Abstract. Paracancerous tissues actively communicate with the tumor and undergo molecular alterations associated with tumorigenesis. Apparent diffusion coefficient (ADC) can help distinguish between rectal adenocarcinoma (RA), tumor-adjacent and tumor-distant tissues. Preoperative determining optimal distal resection margin (DRM) is crucial for formulating surgical options. The present study aimed to assess ADC differences between RA and 1 cm-layer distal paracancerous tissues, providing a potential reference basis for preoperatively determining optimal DRM. A total of 110 consecutive patients with mid-high RA undergoing preoperative diffusion-weighted imaging were included. ADCs of RA and distal paracancerous tissues located ~1, 2 and 3 cm from the tumor margin (defined as D_1, D_2 and D_3, respectively) were measured using five b-value pairs (0 and 50; 0 and 100; 0 and 800; 0 and 1,000; and 0 and 1,500 sec/mm^2). Differences in ADCs between RA, D_1, D_2 and D_3 were compared using the Friedman test with a post hoc Bonferroni correction. Variables that demonstrated statistical differences in multiple pairwise comparisons underwent receiver operating characteristic (ROC) analysis to assess diagnostic performance of ADCs in distinguishing between tissues. ADC at all b-value pairs demonstrated satisfactory performance in distinguishing RA from D_1, D_2 and D_3 [areas under the ROC curves (AUCs), 0.838 to 0.996)]. When the maximum b-value was ≥800 sec/mm^2, the ADC of D_1 was significantly lower compared with those of D_2 and D_3 ($P<0.001$). ADC exhibited an optimal performance in differentiating D_1 from D_2 at b-values of 0 and 800 sec/mm^2, and D_1 from D_3 at b-values of 0 and 1,000 sec/mm^2 (AUCs: 0.652 and 0.692, respectively). However, ADCs of D_2 and D_3 demonstrated no differences at all b-value pairs (all $P>0.05$). In conclusion, ADC may distinguish RA from D_1, D_2 and D_3, and D_1 from D_2/D_3, but cannot distinguish between D_2 and D_3.

Introduction

Colorectal cancer is ranked as the third most prevalent malignancy globally and the second leading cause of cancer-related mortality. Rectal cancer alone contributes to approximately one-third of these cases, with adenocarcinoma comprising >90% (1-3). Total mesorectal excision remains the standard surgical procedure for resectable rectal cancer (4). Despite undergoing curative resection, there is still a recurrence rate of 5-10%, with the distal resection margin (DRM) serving a crucial role (5-7). It has been reported that histologically normal tissues adjacent to tumors undergo molecular alterations associated with tumorigenesis, which can be attributed to field cancerization (8,9). If the tissue exhibiting a precancerous state is not surgically excised, it has the potential to progress into invasive cancer (10). In rectal cancer surgery, an insufficient length of DRM is often associated with a high recurrence rate (5), whilst an excessive length of DRM may result in inadequate remaining rectum and increase the risk of postoperative complications (6). Therefore, it is important to preoperatively determine the optimal DRM for formulating surgical options.

The apparent diffusion coefficient (ADC), derived from the signal intensity of diffusion-weighted imaging (DWI), quantitatively evaluates the mobility of water molecules and indirectly reflects the biological characteristics of tissues (11-13). In general, the presence of low ADC values

Correspondence to: Professor Tian-Wu Chen, Department of Radiology, The Second Affiliated Hospital of Chongqing Medical University, 74 Linjiang Road, Yuzhong, Chongqing 400010, P.R. China
E-mail: tianwuchen_nsmc@163.com; chentw@hospital.cqmu.edu.cn

Abbreviations: ADC, apparent diffusion coefficient; DWI, diffusion-weighted imaging; MRI, magnetic resonance imaging; T2W, T2-weighted; RA, rectal adenocarcinoma; D_1, distal paracancerous tissue located ~1 cm from the tumor margin; D_2, distal paracancerous tissue located ~2 cm from the tumor margin; D_3, distal paracancerous tissue located ~3 cm from the tumor margin; DRM, distal resection margin; DTM, distal tumor margin; ROI, region of interest; ICC, intraclass correlation coefficient; ROC, receiver operating characteristic; AUC, area under the receiver operating characteristic curve; pT, pathological tumor stage; pN, pathological lymph node stage

Key words: DWI, ADC, RA, paracancerous tissue, DRM

indicates a restriction in the diffusion of water molecules, which is commonly observed in several pathological conditions, such as inflammatory, fibrotic or neoplastic processes (11,14). It has been reported that an increase in both the mobility and quantity of water molecules during the transition from normal cells to cancerous cells leads to differences in water molecule diffusion within tissues at different stages of tumorigenesis (15). In addition, stem cells derived from adjacent tissues of the tumor have the potential to induce fibrosis and an inflammatory response (16), thereby affecting the ADC values of paracancerous tissues.

Chen *et al* (17) reported that ADC can be used to differentiate between tumor tissues, tumor-adjacent tissues and tumor-distant tissues in rectal adenocarcinoma (RA); however, the investigation of distal paracancerous tissues only involved the tissues located ~1 and 2 cm from the tumor margin. Currently, there is no exact standard for the length of DRM (18-20), to the best of our knowledge. Therefore, the aim of the present study was to evaluate differences in ADC values of resectable mid-high RA and distal paracancerous tissues located at several distances from the tumor margin in detail, providing a potential reference basis for preoperatively determining the optimal DRM.

Materials and methods

Patients. The study protocol was approved by the Institutional Review Board of the Affiliated Hospital of North Sichuan Medical College (Nanchong, China; approval no. 2024ER219-1), and the requirement for informed consent was waived owing to the retrospective nature of the present study.

From January 2017 to December 2022, clinical and imaging data from 129 consecutive patients with resectable RA who underwent preoperative pelvic magnetic resonance imaging (MRI) scans were collected from The Affiliated Hospital of North Sichuan Medical College (Nanchong, China). Inclusion criteria were as follows: i) Multi-b-value DWI sequences performed within 2 weeks prior to surgery; ii) no cancer-related treatment administered before undergoing multiple b-values DWI; iii) adenocarcinoma confirmed by pathology; and iv) the distal tumor margin (DTM) was positioned ≥3 cm above the dentate line, as the dentate line represents the transition between rectal columnar mucosa and anal squamous mucosa (21), which can result in significant variations in ADC values of the intestinal wall below and above it. Exclusion criteria were as follows: i) No visible tumors on MRI images (n=2); ii) tumors confirmed as mucinous adenocarcinoma, attributing to their high ADC resulting from the abundant mucinous content (n=5); iii) unsatisfactory image quality due to susceptibility or movement artifacts (n=7); iv) abnormal edema exhibited in the intestinal wall, leading to elevated ADC values (n=3); and v) incomplete MRI images or clinical records of patients (n=2). Finally, a total of 110 patients (62 male and 48 female patients; median age, 66 years; age range, 28-84 years) with RA confirmed by pathology were included in the present study for analysis.

All patients with RA underwent pelvic MRI including DWI 2 weeks before radical resection with regional lymph node dissection. The tumor differentiation, pathological tumor stage (pT) and pathological lymph node stage (pN) for rectal cancer were determined based on the postoperative histopathological examination. Tumors located within 15 cm from the DTM to the anal verge were categorized as rectal neoplasms, further classified into low (0-5 cm), middle (>5-10 cm) and high (>10-15 cm) rectal tumors based on their respective distances from the DTM to the anal verge (22). As the distance from the dentate line to the anal verge was 2-3 cm (21), and DTM was required to be >3 cm above the dentate line in the present study, patients with mid-high RA were included.

MRI techniques. For each enrolled patient, imaging was performed using a 3.0 Tesla scanner (Discovery™ MR750; GE Healthcare) with a 32-channel phased-array torso coil in the pelvic region. The imaging sequences included axial T_2-weighted (T_2W) fast-recovery fast spin-echo with fat suppression sequence, sagittal T_2W Propeller with fat suppression sequence, axial multi-b-value (0, 50, 100, 800, 1,000 and 1,500 sec/mm^2) DWI based on echo-planar imaging sequence. The parameters of all sequences are listed in Table I. The patients were positioned in a supine posture during the scanning procedure. The scanning range was from the level of the lumbar 4-5 intervertebral disc to 10 cm below the pubic symphysis, ensuring coverage of the entire rectum.

Image analysis. DWI data were transferred to the Advantage Workstation (version 4.5; GE Healthcare), and ADC maps were automatically generated using the post-processing Functool software (version 10.4.04; GE Healthcare). All images were independently evaluated by two abdominal radiologists (radiologist 1 and radiologist 2, with 7 and 3 years of experience in this field, respectively), and any disagreements were resolved by another expert with 26 years of experience. The expert and two radiologists were blinded to the clinical and histopathology information of patients, except for the diagnosis of RA.

The ADC maps and values were derived from DWI using five different b-value pairs (0 and 50; 0 and 100; 0 and 800; 0 and 1,000; and 0 and 1,500 sec/mm^2) based on the mono-exponential model formula: $ADC=\ln(S_0/S_1)/(b_1-b_0)$, where b represents the diffusion gradient value and S_0 and S_1 denote the signal intensity of tissue on DWI at b_0 and b_1, respectively (12,17). The Japanese guidelines recommend a DRM of ≥3 cm for rectal cancer located above the peritoneal reflection and 2 cm for those below it (19). Moreover, there have been very few reports of distal tumor infiltration extending <3 cm (5). Thus, a DRM of 3 cm is generally considered a safe resection margin for patients with rectal cancer. Subsequently, ADC measurements were performed on RA and three distal paracancerous tissues located at ~1 (D_1), ~2 (D_2) and ~3 cm (D_3) from the DTM.

In the present study, the ADCs of RA, D_1, D_2 and D_3 were measured using the single-slice region of interest (ROI) method. Firstly, location of RA was determined based on the T_2W and DWI images, where the tumor presented as an irregular thickening of the intestinal wall with isointense or hyperintense signal on the T_2W image and hyperintense signal on the DWI image (Fig. 1A-C). Secondly, the locations of D_1, D_2 and D_3 were determined based on the sagittal T_2W images (Fig. 1B), whilst the axial DWI images of D_1, D_2 and D_3 were captured at the corresponding locations. Thirdly, on the axial high b-value DWI image, the maximum cross-section of the

Table I. Scan parameters of the magnetic resonance imaging sequences.

Parameter	Axial T_2W imaging	Sagittal T_2W imaging	Axial multi-b-value DWI[a]
Repetition time, msec	5,050	7,570	3,225
Echo time, msec	120	60	57
Flip angle, °	111	140	90
Field of view, cm	36x36	36x36	38x30
Slice thickness, mm	5	5	5
Intersection gap, mm	1	1	1
Matrix	384x256	320x320	128x192
Number of excitations	2	3	1/2/4

[a]DWI was performed using b-values of 0, 50, 100, 800, 1,000 and 1,500 sec/mm^2 with corresponding numbers of excitations of 1, 2, 2, 4, 4 and 4 respectively. T_2W, T_2 weighted; DWI, diffusion-weighted imaging.

tumor was selected and an ROI was delineated along the tumor margin whilst carefully excluding necrotic, fatty and vascular regions (Fig. 1C). In accordance with the method described in a previously published report (17), ROIs of D_1, D_2 and D_3 were delineated to cover more than a semicircle of the rectal wall, and the surrounding adipose tissue, blood vessels and luminal gas were excluded (Fig. 1D). After delineating the ROIs for the tumor, D_1, D_2 and D_3 on axial high b-value DWI images, corresponding ROIs were automatically generated on the ADC maps to obtain ADC values for each region (Fig. 1E and F). The ADC measurement was repeated three times for each tissue, and the final value was determined by calculating the average of these three measurements. Additionally, the ADCs of RA, D_1, D_2 and D_3 were independently measured by the aforementioned two radiologists to evaluate the interobserver agreement.

Statistical analysis. Statistical analyses were performed using SPSS software (version 25; IBM Corp.). P<0.05 was considered to indicate a statistically significant difference. The intraclass correlation coefficient (ICC) was used to assess the interobserver agreements for each ADC measurement. The ICC was classified into poor (0-0.20), fair (0.21-0.40), moderate (0.41-0.60), good (0.61-0.80) and excellent (0.81-1.00) agreements (23). If the agreement was good or excellent, the measurements of radiologist 1 were used for subsequent analysis. If the agreement was unsatisfactory, the average of the measurements taken by two radiologists (radiologist 1 and radiologist 2) were used for subsequent analysis.

The ADCs of RA, D_1, D_2 and D_3 were compared using the Friedman test. In cases where the P-values indicated statistically significant differences, post hoc multiple pairwise comparisons between different tissues were performed using the Bonferroni correction test. The results were visually represented using boxplots. Subsequently, variables that demonstrated statistically significant differences in pairwise comparisons underwent receiver operating characteristic (ROC) analysis to assess the efficacy of ADCs in distinguishing between different tissues. In addition, considering that advanced-stage RA may have more cell proliferation compared with early-stage RA, and there may be differences in the length of safe DRM between the two stages, the Mann-Whitney U test was used to analyze the ADCs of different tissues between pT1-2 and pT3-4 stages.

Results

Patient characteristics. A total of 110 patients with RA were included in the present study, comprising 62 (56.4%) male patients and 48 (43.6%) female patients. The median age was 66 years (range, 28-84 years). There were 31 (28.2%) tumors located in the high rectum and 79 (71.8%) tumors located in the middle rectum. The tumor differentiation was observed as well-differentiated adenocarcinoma in 39 (35.4%) patients, moderately differentiated adenocarcinoma in 65 (59.1%) patients and poorly differentiated adenocarcinoma in 6 (5.5%) patients. Regarding the pathological stage, there were 27 (24.5%) patients classified as pT1-2 and 83 (75.5%) patients classified as pT3-4. Additionally, there were 65 (59.1%) patients classified as pN0 and 45 (40.9%) patients classified as pN1-2.

Interobserver agreements of ADCs at different b-value pairs. The interobserver agreements for the ADC values of RA, D_1, D_2 and D_3 are presented in Table II. The interobserver agreements for the ADC values at different b-value pairs were excellent (all ICCs >0.80). Therefore, the measurements obtained by radiologist 1 were used for subsequent analysis.

Comparisons of ADCs between RA, D_1, D_2 and D_3. The ADC values of RA, D_1, D_2 and D_3 obtained from different b-value pairs are summarized in Table III. The Friedman test demonstrated significant differences in ADCs between the four different tissues at all b-value pairs (all P<0.001). Post hoc multiple pairwise comparisons using the Bonferroni correction test were performed to further assess the differences in ADCs between different tissues (Fig. 2). The tumor exhibited lower ADC values compared with D_1, D_2 and D_3 at all b-value pairs (all P<0.001). Furthermore, at b-value pairs with the maximum b-value of ≥800 sec/mm^2 (0 and 800; 0 and 1,000; and 0 and 1,500 sec/mm^2), the ADC of D_1 was significantly lower compared with those of both D_2 and D_3 (P<0.001). However, no significant differences in ADCs were observed between D_1, D_2 and D_3 at b-value pairs with the maximum b-value of ≤100 sec/mm^2 (0 and 50, and 0 and 100 sec/mm^2; P>0.05).

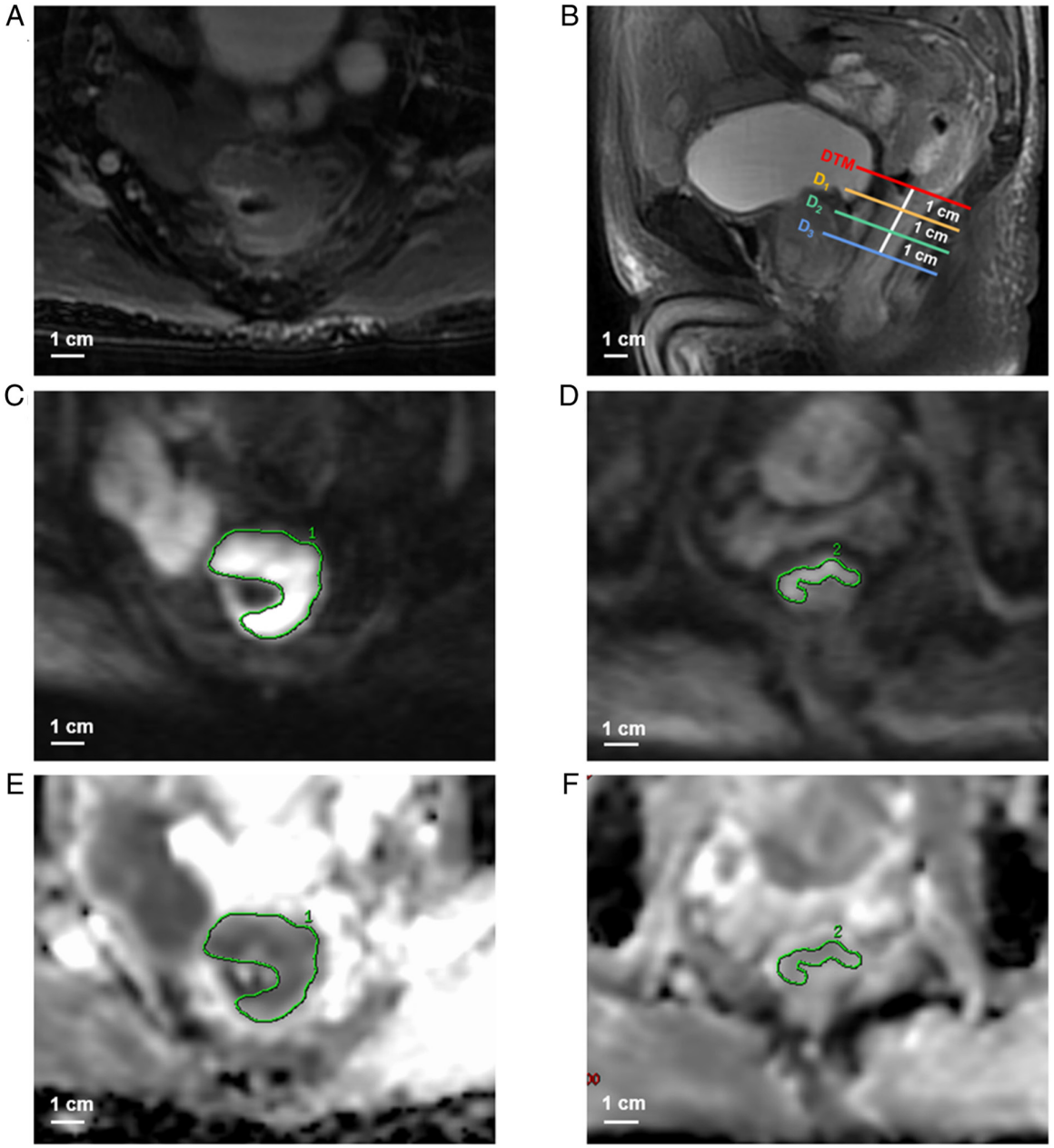

Figure 1. Measurement of the ADC values of the tumor and distal paracancerous tissues in a 73-year-old male patient with pT3-staged adenocarcinoma of the middle rectum. (A) Axial T_2-weighted image shows the tumor is presented as an irregular thickening of rectal wall. (B) Sagittal T_2-weighted image (red line, DTM; orange line, D_1; green line, D_2; blue line, D_3). ROIs for the (C) tumor on the largest tumor cross-section and (D) D_1, which covers more than a semicircle of the rectal wall, were manually delineated on axial diffusion-weighted images (b=1,000 sec/mm^2). Subsequently, ROIs for the (E) tumor and (F) D_1 were automatically generated on the corresponding ADC maps (b=0 and 1,000 sec/mm^2) to obtain ADC values for each region. The ADC values of the tumor and D_1 were 1.160x10^{-3} mm^2/sec and 1.530x10^{-3} mm^2/sec, respectively. ADC measurements for D_2 and D_3 were performed in a consistent manner with that used for D_1. ADC, apparent diffusion coefficient; D_1, distal paracancerous tissue located ~1 cm from the tumor margin; D_2, distal paracancerous tissue located ~2 cm from the tumor margin; D_3, distal paracancerous tissue located ~3 cm from the tumor margin; DTM, distal tumor margin; ROI, region of interest; pT, pathological tumor stage.

There were no significant differences in ADCs between D_2 and D_3 at all b-value pairs (all P>0.05).

ADCs of RA, D_1, D_2 and D_3 between different pT stages. The ADC values of RA, D_1, D_2 and D_3 obtained from different b-value pairs at pT1-2 and pT3-4 stages are summarized in Table IV. Only when b=0 and 1,000 sec/mm^2, and b=0 and 1,500 sec/mm^2, the ADC values of pT1-2 staged tumors were significantly higher compared with those of pT3-4 staged tumors (P<0.05). However, no statistically significant differences in ADC values between tumors with different pathological stages were demonstrated at the other b-value pairs (P>0.05). Furthermore, there were no statistically significant differences in ADC values of D_1, D_2 and D_3 between tumors with different pathological stages at all b-value pairs (all P>0.05). Therefore, further subgroup analysis was not performed.

ROC analyses of ADCs for differentiation between RA, D_1, D_2 and D_3. The efficacy of ADCs in distinguishing between different tissues was assessed using ROC analysis for variables

Table II. Evaluation of interobserver agreements for apparent diffusion coefficient values of the tumor, distal paracancerous tissue located ~1, 2 and 3 cm from the tumor margin at different b-value pairs.

b-value, sec/mm^2	Interobserver intraclass correlation coefficient (95% CI)			
	Tumor	D_1	D_2	D_3
0 and 50	0.915 (0.875-0.942)	0.876 (0.820-0.915)	0.894 (0.845-0.928)	0.867 (0.810-0.908)
0 and 100	0.832 (0.764-0.882)	0.904 (0.858-0.935)	0.885 (0.827-0.923)	0.878 (0.815-0.919)
0 and 800	0.896 (0.844-0.930)	0.924 (0.887-0.949)	0.933 (0.900-0.955)	0.913 (0.869-0.942)
0 and 1,000	0.927 (0.865-0.957)	0.929 (0.895-0.952)	0.951 (0.928-0.967)	0.943 (0916-0.961)
0 and 1,500	0.900 (0.852-0.932)	0.910 (0.870-0.937)	0.916 (0.879-0.942)	0.927 (0.895-0.950)

CI, confidence interval; D_1, distal paracancerous tissue located ~1 cm from the tumor margin; D_2, distal paracancerous tissue located ~2 cm from the tumor margin; D_3, distal paracancerous tissue located ~3 cm from the tumor margin.

Table III. Comparison of apparent diffusion coefficients between the tumor, distal paracancerous tissue located ~1, 2 and 3 cm from the tumor margin at different b-value pairs.

b-value, sec/mm^2	Median ADC (25% quantile, 75% quantile), x10^{-3} mm^2/sec				
	Tumor	D_1	D_2	D_3	P-value
0 and 50	2.080 (1.473, 2.589)	3.148 (2.598, 3.645)	3.244 (2.598, 3.783)	3.224 (2.645, 3.840)	<0.001
0 and 100	1.825 (1.382, 2.064)	2.527 (2.113, 3.059)	2.557 (2.187, 3.070)	2.587 (2.173, 2.965)	<0.001
0 and 800	1.083 (1.028, 1.141)	1.505 (1.389, 1.623)	1.584 (1.500, 1.764)	1.625 (1.495, 1.730)	<0.001
0 and 1,000	1.003 (0.942, 1.051)	1.405 (1.269, 1.538)	1.514 (1.377, 1.661)	1.552 (1.400, 1.647)	<0.001
0 and 1,500	0.887 (0.852, 0.937)	1.247 (1.126, 1.368)	1.312 (1.230, 1.443)	1.347 (1.246, 1.430)	<0.001

ADC, apparent diffusion coefficient; D_1, distal paracancerous tissue located ~1 cm from the tumor margin; D_2, distal paracancerous tissue located ~2 cm from the tumor margin; D_3, distal paracancerous tissue located ~3 cm from the tumor margin.

that showed statistically significant differences, based on the aforementioned results. This analysis yielded several metrics, including the cut-off value, sensitivity, specificity, accuracy and area under the ROC curve (AUC), which are presented in Table V. ADCs at the maximum b-value of ≥800 sec/mm^2 exhibited superior discriminatory capability in distinguishing RA from D_1 (Fig. 3A), RA from D_2 (Fig. 3B) and RA from D_3 (Fig. 3C) compared with those at the maximum b-value of ≤100 sec/mm^2. Particularly at b-values of 0 and 1,500 sec/mm^2, ADC cut-off values of 1.009x10^{-3} mm^2/sec, 1.050x10^{-3} mm^2/sec and 1.070x10^{-3} mm^2/sec demonstrated superior ability in distinguishing RA from D_1, from D_2 and from D_3 (AUCs: 0.982, 0.992 and 0.996, respectively). Additionally, ADC cut-off values of 1.522x10^{-3} mm^2/sec (b=0 and 800 sec/mm^2) and 1.539x10^{-3} mm^2/sec (b=0 and 1000 sec/mm^2) exhibited optimal diagnostic performance in differentiating D_1 from D_2 (AUC, 0.652; Fig. 4A) and D_1 from D_3 (AUC, 0.692; Fig. 4B).

Discussion

In the present study, the disparities in ADCs between RA and distal paracancerous tissues (~1, 2 and 3 cm from the tumor margin) were evaluated, and the diagnostic performance of ADCs in distinguishing between these tissues was assessed.

As demonstrated in the present study, the tumor exhibited lower ADC values compared with distal paracancerous tissues at all b-value pairs, which was consistent with the results of a previous study (17). A possible explanation for this finding is the higher cellular density and irregular cell morphology within the tumor, which results in narrower and distorted intercellular spaces that restrict the diffusion of water molecules (24,25). Consequently, the tumor exhibits lower ADC values compared with D_1, D_2 and D_3. Furthermore, the present study demonstrated that ADCs at the maximum b-values of ≥800 sec/mm^2 (AUCs, 0.963 to 0.996) exhibited superior discriminatory capability in distinguishing the tumor from distal paracancerous tissues compared with those at the maximum b-values of ≤100 sec/mm^2 (AUCs, 0.838 to 0.843). Particularly at b-values of 0 and 1,500 sec/mm^2, ADC demonstrated optimal diagnostic efficacy in distinguishing RA from D_1, D_2 and D_3 (AUCs, 0.982 to 0.996). The results may be due to the fact that when calculating ADC at the higher maximum b-values, it predominantly reflects the diffusion of water molecules; conversely, when computing ADC at the lower maximum b-value, it primarily reflects microcapillary perfusion (26).

Diffusion and perfusion are distinct physical and biological phenomena, both serving as indicators for

Table IV. Comparison of apparent diffusion coefficients of the tumor, distal paracancerous tissue located ~1, 2 and 3 cm from the tumor margin between different pathological tumor stages.

b-value, sec/mm^2	Tissue	Median ADC (25% quantile, 75% quantile), x10^{-3} mm^2/sec		
		pT1-2 (n=27)	pT3-4 (n=83)	P-value
0 and 50	Tumor	2.110 (1.533, 2.683)	2.053 (1.440, 2.550)	0.518
	D_1	3.210 (2.717, 3.667)	3.080 (2.553, 3.637)	0.451
	D_2	3.277 (2.710, 3.793)	3.220 (2.563, 3.780)	0.654
	D_3	3.123 (2.677, 3.953)	3.293 (2.540, 3.837)	0.870
0 and 100	Tumor	1.900 (1.427, 2.257)	1.783 (1.377, 2.033)	0.202
	D_1	2.633 (2.220, 3.097)	2.497 (2.047, 3.055)	0.485
	D_2	2.737 (2.317, 2.923)	2.517 (2.023, 3.297)	0.534
	D_3	2.630 (2.373, 2.933)	2.560 (2.083, 3.100)	0.710
0 and 800	Tumor	1.107 (1.050, 1.193)	1.080 (1.017, 1.133)	0.090
	D_1	1.540 (1.410, 1.723)	1.490 (1.373, 1.600)	0.198
	D_2	1.523 (1.420, 1.780)	1.600 (1.520, 1.763)	0.406
	D_3	1.630 (1.440, 1.717)	1.623 (1.500, 1.73)	0.797
0 and 1,000	Tumor	1.023 (0.980, 1.113)	0.989 (0.929, 1.040)	0.006
	D_1	1.493 (1.223, 1.580)	1.397 (1.270, 1.533)	0.380
	D_2	1.510 (1.377, 1.677)	1.523 (1.383, 1.653)	0.800
	D_3	1.500 (1.397, 1.637)	1.553 (1.413, 1.663)	0.555
0 and 1,500	Tumor	0.909 (0.864, 0.974)	0.879 (0.847, 0.929)	0.041
	D_1	1.300 (1.097, 1.400)	1.243 (1.127, 1.340)	0.240
	D_2	1.390 (1.190, 1.480)	1.300 (1.233, 1.410)	0.397
	D_3	1.343 (1.250, 1.423)	1.347 (1.243, 1.430)	0.947

ADC, apparent diffusion coefficient; pT, pathological tumor stage; D_1, distal paracancerous tissue located ~1 cm from the tumor margin; D_2, distal paracancerous tissue located ~2 cm from the tumor margin; D_3, distal paracancerous tissue located ~3 cm from the tumor margin.

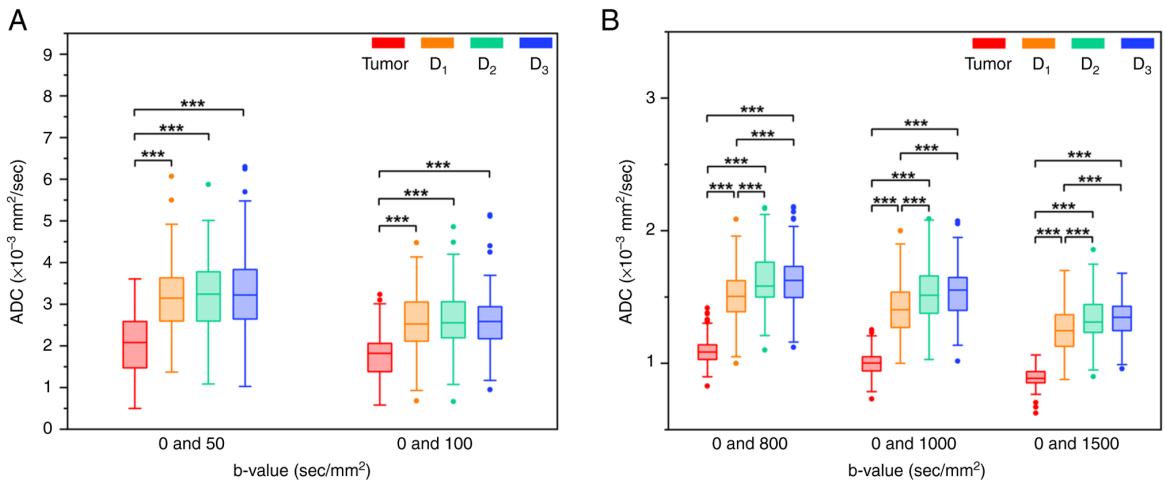

Figure 2. Multiple pairwise comparisons of ADCs at different b-value pairs between the tumor, D_1, D_2 and D_3. Comparisons of ADCs at the maximum b-value of (A) ≤100 sec/mm^2 and (B) ≥800 sec/mm^2 between the tumor, D_1, D_2 and D_3. The boxes represent the interquartile range, and the lines inside the box indicate the median; whiskers denote the lowest and highest values within 1.5 times the interquartile range; dots indicate outliers; and asterisks indicate significant differences between the tissues assessed using Friedman test with Bonferroni correction ***P<0.001. ADC, apparent diffusion coefficient; D_1, distal paracancerous tissue located ~1 cm from the tumor margin; D_2, distal paracancerous tissue located ~2 cm from the tumor margin; D_3, distal paracancerous tissue located ~3 cm from the tumor margin.

several physiological or pathological processes (25). The diffusion coefficient has been reported to be a more effective diagnostic parameter than the perfusion coefficient in distinguishing the tumor from paracancerous tissue (27). Additionally, the findings of the present study indicated that the ADC values of pT1-2 staged tumors were significantly

Table V. Receiver operating characteristic curve analyses of apparent diffusion coefficients for the differentiation between the tumor and distal paracancerous tissue located ~1, 2 and 3 cm from the tumor margin at different b-value pairs.

A, Tumor vs. D_1

b-value, sec/mm^2	Cut-off value, x10^{-3} mm^2/sec	Sensitivity	Specificity	Accuracy	AUC (95% CI)
0 and 50	2.714	0.827	0.727	0.777	0.842 (0.790-0.894)
0 and 100	2.277	0.891	0.673	0.782	0.838 (0.784-0.891)
0 and 800	1.329	0.964	0.855	0.909	0.963 (0.939-0.987)
0 and 1,000	1.117	0.909	0.973	0.941	0.981 (0.966-0.995)
0 and 1,500	1.009	0.936	0.955	0.945	0.982 (0.967-0.997)

B, Tumor vs. D_2

b-value, sec/mm^2	Cut-off value, x10^{-3} mm^2/sec	Sensitivity	Specificity	Accuracy	AUC (95% CI)
0 and 50	2.960	0.955	0.645	0.800	0.843 (0.790-0.895)
0 and 100	2.275	0.891	0.727	0.809	0.840 (0.786-0.894)
0 and 800	1.339	0.973	0.909	0.941	0.987 (0.976-0.997)
0 and 1,000	1.167	0.936	0.982	0.959	0.990 (0.980-1.000)
0 and 1,500	1.050	0.982	0.945	0.964	0.992 (0.983-1.000)

C, Tumor vs. D_3

b-value, sec/mm^2	Cut-off value, x10^{-3} mm^2/sec	Sensitivity	Specificity	Accuracy	AUC (95% CI)
0 and 50	2.932	0.936	0.636	0.786	0.842 (0.790-0.895)
0 and 100	2.158	0.818	0.764	0.791	0.839 (0.785-0.893)
0 and 800	1.340	0.973	0.927	0.950	0.989 (0.980-0.998)
0 and 1,000	1.220	0.982	0.964	0.973	0.994 (0.986-1.000)
0 and 1,500	1.070	1.000	0.945	0.973	0.996 (0.991-1.000)

D, D_1 vs. D_2

b-value, sec/mm^2	Cut-off value, x10^{-3} mm^2/sec	Sensitivity	Specificity	Accuracy	AUC (95% CI)
0 and 800	1.522	0.582	0.682	0.632	0.652 (0.580-0.724)
0 and 1,000	1.425	0.564	0.682	0.623	0.651 (0.578-0.723)
0 and 1,500	1.249	0.509	0.709	0.609	0.617 (0.543-0.691)

E, D_1 vs. D_3

b-value, sec/mm^2	Cut-off value, x10^{-3} mm^2/sec	Sensitivity	Specificity	Accuracy	AUC (95% CI)
0 and 800	1.559	0.636	0.673	0.655	0.674 (0.603-0.745)
0 and 1,000	1.539	0.755	0.536	0.645	0.692 (0.623-0.761)
0 and 1,500	1.249	0.509	0.745	0.627	0.658 (0.586-0.729)

AUC, area under receiver operating characteristic curve; CI, confidence interval; D_1, distal paracancerous tissue located ~1 cm from the tumor margin; D_2, distal paracancerous tissue located ~2 cm from the tumor margin; D_3, distal paracancerous tissue located ~3 cm from the tumor margin.

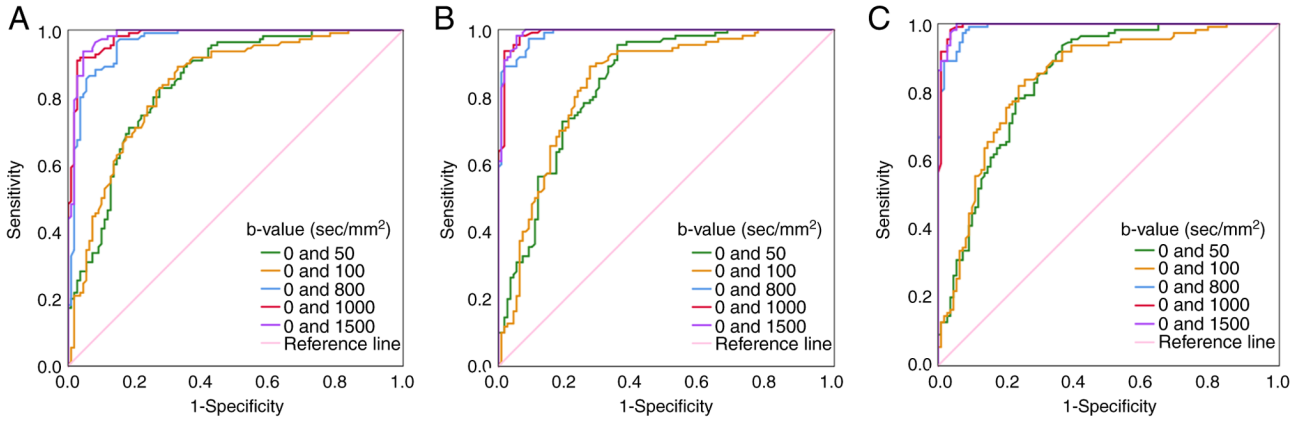

Figure 3. ROC analyses of ADCs at different b-value pairs to differentiate the tumor from D_1, D_2 and D_3. Differentiation of the tumor from (A) D_1, (B) D_2 and (C) D_3. These ROC curves demonstrate that the ADCs at the maximum b-value of ≥800 sec/mm^2 can differentiate the tumor from distal paracancerous tissues more effectively compared with the ADCs at the maximum b-value of ≤100 sec/mm^2. ROC, receiver operating characteristic curve; ADC, apparent diffusion coefficient; D_1, distal paracancerous tissue located ~1 cm from the tumor margin; D_2, distal paracancerous tissue located ~2 cm from the tumor margin; D_3, distal paracancerous tissue located ~3 cm from the tumor margin.

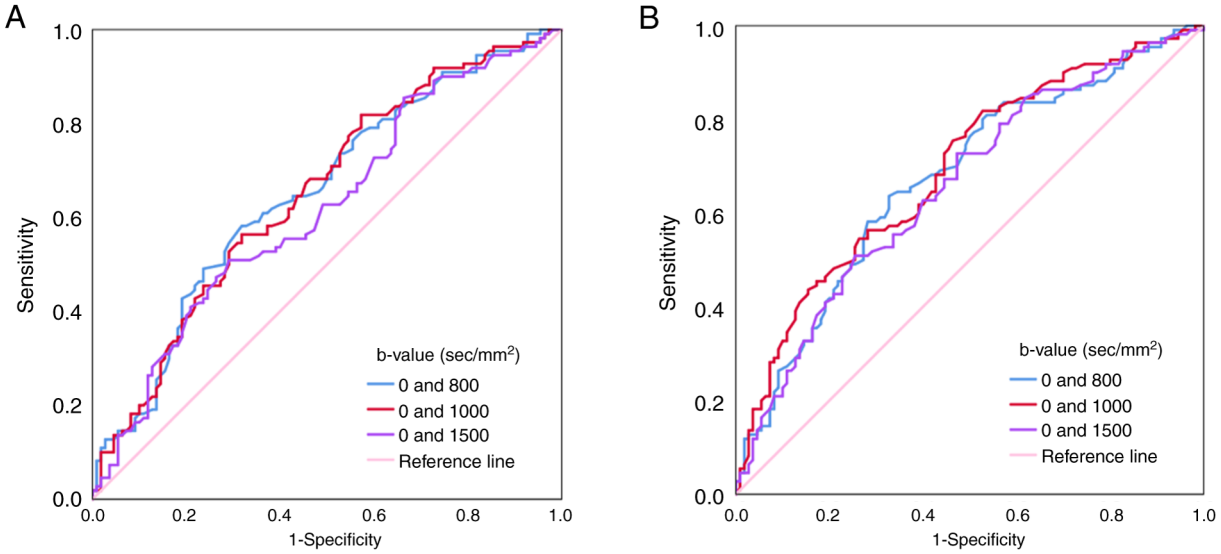

Figure 4. Receiver operating characteristic curve analyses of apparent diffusion coefficients at the maximum b-value of ≥800 sec/mm^2 to differentiate D_1 from D_2 and D_3. Differentiation of D_1 from (A) D_2 and (B) D_3. D_1, distal paracancerous tissue located ~1 cm from the tumor margin; D_2, distal paracancerous tissue located ~2 cm from the tumor margin; D_3, distal paracancerous tissue located ~3 cm from the tumor margin.

higher compared with those of pT3-4 staged tumors at certain b-value pairs (b=0 and 1,000 sec/mm^2, and b=0 and 1,500 sec/mm^2), which is consistent with previous studies (28,29). This may be due to the increased density of tumor cells and reduced extracellular space as the tumor progresses, leading to greater restriction of water molecule diffusion.

In the present study, the ADC of D_1 was lower compared with those of D_2 and D_3 at the maximum b-values of ≥800 sec/mm^2. Chen *et al* (17) also reported a decrease in ADC values of D_1 compared with D_2 in their assessment of distal paracancerous tissues, but the ADC values between D_1/D_2 and D_3 were not compared and cases of lower rectal cancer were not excluded. The result of the present study may be attributed to molecular alterations during tumorigenesis that can lead to abnormal increases in water molecule mobility and quantity (15). In addition, the molecular alterations associated with tumorigenesis are more pronounced in paracancerous tissues located closer to the tumor compared with tumor-distant tissues (8,9). Furthermore, previous research has demonstrated that the more severe the intestinal inflammation and fibrosis, the lower the ADC value (30). Stem cells derived from the adjacent tissues of the tumor have the potential to induce fibrosis and an inflammatory response (16), indicating that inflammation and fibrosis are more pronounced in paracancerous tissues located closer to the tumor compared with tumor-distant tissues. Hence, the diffusion of water molecules is more restricted in D_1 compared with D_2 and D_3. However, there were no significant differences in ADCs at the maximum b-value of ≤100 sec/mm^2 between D_1, D_2 and D_3 in the present study. This may be because microcapillary perfusion cannot accurately discern the subtle differences within these tissues.

Currently, there is no exact standard on DWI for the definition of the length of DRM. The present study demonstrated that there were no significant differences in ADCs between D_2 and D_3 at all b-value pairs, suggesting that D_2 and D_3 may possess similar biological characteristics, such as microstructure, cell sequencing and tissue composition. Therefore, we hypothesize that the safe DRM in mid-high RA surgery may be reduced to 2 cm. According to the National Comprehensive Cancer Network guidelines, patients with mid-high rectal cancer are recommended to have a DRM length of 4-5 cm (20). Japanese guidelines recommend a minimum distance of 3 cm for DRM in cases of rectal cancer located above the peritoneal reflection and 2 cm for those below it (19). Furthermore, there have been very few reports of distal tumor infiltration extending <3 cm (5). From a clinical perspective, a DRM of 3 cm is generally considered a safe resection margin for patients with rectal cancer. A previous metabolomic study by Zhang *et al* (18) may support the finding of the present study, which also suggests that a DRM of 2 cm may be considered as a safe resection margin. With the advancement of medical technology, the length of DRM in rectal cancer surgery has been progressively reduced. Manegold *et al* (31) reported that R0 resection of rectal cancer following preoperative chemoradiotherapy achieved excellent outcomes, even with DRM <1 cm, without impacting recurrence-free survival of patients. However, a meta-analysis reported that for patients with rectal cancer undergoing surgery alone, DRM <1 cm may not be deemed safe (32).

In addition, the results of the present further indicated that the ADCs at the maximum b-values of ≥800 sec/mm^2 exhibited a certain diagnostic value in discriminating between D_1 and D_2/D_3 (AUCs, 0.617 to 0.692). The ADCs at b-values of 0 and 800 sec/mm^2 or b-values of 0 and 1,000 sec/mm^2 demonstrated improved diagnostic performance in differentiating between D_1 and D_2 (AUC, 0.652 or 0.651), and the ADC at b-values of 0 and 1,000 sec/mm^2 exhibited optimal diagnostic performance in differentiating between D_1 and D_3 (AUC, 0.692). Although ADC could not achieve an excellent diagnostic performance in distinguishing between D_1 and D_2/D_3, it may still have clinical importance for preoperative surgical decision-making in resectable mid-high RA.

The present study has several limitations. Firstly, it was a single-center retrospective study, and a prospective study across multiple institutions and scanners is needed to validate the findings. Secondly, patients with RA who had not undergone preoperative chemoradiotherapy were assessed, and further studies are needed for patients who have undergone this therapy. Thirdly, the results of the present investigation on distal paracancerous tissues located at several distances from the tumor margin has not been verified by comprehensive comparison with the corresponding histopathology and molecular alterations of these tissues. Relevant research should be performed in the future to support the findings of the present study.

In conclusion, the results of the present study demonstrated that there were differences in ADCs between RA, D_1 and D_2/D_3, and ADC could distinguish RA from D_1, D_2 and D_3, and differentiate D_1 from D_2/D_3 to a certain degree. However, no significant differences were demonstrated in ADCs between D_2 and D_3, indicating that they may possess similar biological characteristics and that the safe DRM in RA surgery may be reduced to 2 cm. The findings suggest that ADC may potentially serve as a valuable tool for evaluating the optimal distal resection range, contributing to the development of surgical strategies to reduce the risk of local recurrence and postoperative complications.

Acknowledgements

Not applicable.

Funding

No funding was received.

Availability of data and materials

The data generated in the present study may be requested from the corresponding author.

Authors' contributions

TWC, HYZ, XMZ participated in the design of the study. HL, YQG, YSW and HLQ contributed to data analysis. TWC, HL and YQG drafted and revised the article, gave final approval of the version to be published, agreed to the submitted journal and agreed to be accountable for all aspects of the work. TWC, HL and YQG proofread the manuscript. TWC submitted the manuscript. All authors have read and approved the final version of the manuscript. TWC and HL confirm the authenticity of all the raw data.

Ethics approval and consent to participate

The present study was approved by the Ethical Committee of the Affiliated Hospital of North Sichuan Medical College (Nanchong, China; approval no. 2024ER219-1). The ethics committee waived the need for informed consent due to the retrospective nature of the present study.

Patient consent for publication

Not applicable.

Competing interests

The authors declare that they have no competing interests.

References

1. Siegel RL, Wagle NS, Cercek A, Smith RA and Jemal A: Colorectal cancer statistics, 2023. CA Cancer J Clin 73: 233-254, 2023.
2. Sung H, Ferlay J, Siegel RL, Laversanne M, Soerjomataram I, Jemal A and Bray F: Global cancer statistics 2020: GLOBOCAN estimates of incidence and mortality worldwide for 36 cancers in 185 countries. CA Cancer J Clin 71: 209-249, 2021.
3. Islam SMA, Patel R, Bommareddy RR, Khalid KM and Acevedo-Duncan M: The modulation of actin dynamics via atypical protein kinase-C activated cofilin regulates metastasis of colorectal cancer cells. Cell Adh Migr 13: 106-120, 2019.
4. Dekker E, Tanis PJ, Vleugels JLA, Kasi PM and Wallace MB: Colorectal cancer. Lancet 394: 1467-1480, 2019.

5. Kosuge M, Eto K, Sasaki S, Sugano H, Yatabe S, Takeda Y, Ito D, Ohkuma M and Yanaga K: Clinical factors affecting the distal margin in rectal cancer surgery. Surg Today 50: 743-748, 2020.
6. Ekkarat P, Boonpipattanapong T, Tantiphlachiva K and Sangkhathat S: Factors determining low anterior resection syndrome after rectal cancer resection: A study in Thai patients. Asian J Surg 39: 225-231, 2016.
7. Song SH, Park JS, Choi GS, Seo AN, Park SY, Kim HJ, Lee SM and Yoon G: Impact of the distal resection margin on local recurrence after neoadjuvant chemoradiation and rectal excision for locally advanced rectal cancer. Sci Rep 11: 22943, 2021.
8. Trujillo KA, Hines WC, Vargas KM, Jones AC, Joste NE, Bisoffi M and Griffith JK: Breast field cancerization: Isolation and comparison of telomerase-expressing cells in tumor and tumor adjacent, histologically normal breast tissue. Mol Cancer Res 9: 1209-1221, 2011.
9. Guo H, Zeng W, Feng L, Yu X, Li P, Zhang K, Zhou Z and Cheng S: Integrated transcriptomic analysis of distance-related field cancerization in rectal cancer patients. Oncotarget 8: 61107-61117, 2017.
10. Braakhuis BJ, Tabor MP, Kummer JA, Leemans CR and Brakenhoff RH: A genetic explanation of Slaughter's concept of field cancerization: Evidence and clinical implications. Cancer Res 63: 1727-1730, 2003.
11. Chavhan GB and Caro-Dominguez P: Diffusion-weighted imaging in pediatric body magnetic resonance imaging. Pediatr Radiol 46: 847-857, 2016.
12. Subhawong TK, Jacobs MA and Fayad LM: Diffusion-weighted MR imaging for characterizing musculoskeletal lesions. Radiographics 34: 1163-1177, 2014.
13. Ko CC, Yeh LR, Kuo YT and Chen JH: Imaging biomarkers for evaluating tumor response: RECIST and beyond. Biomark Res 9: 52, 2021.
14. Harold KM, MacCuaig WM, Holter-Charkabarty J, Williams K, Hill K, Arreola AX, Sekhri M, Carter S, Gomez-Gutierrez J, Salem G, *et al*: Advances in imaging of inflammation, fibrosis, and cancer in the gastrointestinal tract. Int J Mol Sci 23: 16109, 2022.
15. Marques MPM, Batista de Carvalho ALM, Mamede AP, Dopplapudi A, García Sakai V and Batista de Carvalho LAE: Role of intracellular water in the normal-to-cancer transition in human cells-insights from quasi-elastic neutron scattering. Struct Dyn 7: 05470, 2020.
16. Zhao Y, Guo M, Zhao F, Liu Q and Wang X: Colonic stem cells from normal tissues adjacent to tumor drive inflammation and fibrosis in colorectal cancer. Cell Commun Signal 21: 186, 2023.
17. Chen XQ, Tan BG, Xu M, Zhou HY, Ou J, Zhang XM, Yu ZY and Chen TW: Apparent diffusion coefficient derived from diffusion-weighted imaging to differentiate between tumor, tumor-adjacent and tumor-distant tissues in resectable rectal adenocarcinoma. Eur J Radiol 155: 110506, 2022.
18. Zhang S, Pan G, Liu Z, Kong Y and Wang D: Association of levels of metabolites with the safe margin of rectal cancer surgery: A metabolomics study. BMC Cancer 22: 1043, 2022.
19. Hashiguchi Y, Muro K, Saito Y, Ito Y, Ajioka Y, Hamaguchi T, Hasegawa K, Hotta K, Ishida H, Ishiguro M, *et al*: Japanese society for cancer of the colon and rectum. Japanese society for cancer of the colon and rectum (JSCCR) guidelines 2019 for the treatment of colorectal cancer. Int J Clin Oncol 25: 1-42, 2020.
20. Benson AB, Venook AP, Al-Hawary MM, Azad N, Chen YJ, Ciombor KK, Cohen S, Cooper HS, Deming D, Garrido-Laguna I, *et al*: Rectal cancer, version 2.2022, NCCN clinical practice guidelines in oncology. J Natl Compr Canc Netw 20: 1139-1167, 2022.
21. Liu X, Wang Z, Ren H, Wang Z and Li J: Accuracy of magnetic resonance imaging in defining dentate line in anal fistula. BMC Med Imaging 22: 201, 2022.
22. Kalisz KR, Enzerra MD and Paspulati RM: MRI evaluation of the response of rectal cancer to neoadjuvant chemoradiation therapy. Radiographics 39: 538-556, 2019.
23. Ye Z, Yao S, Yang T, Li Q, Li Z and Song B: Abdominal diffusion-weighted MRI with simultaneous multi-slice acquisition: Agreement and reproducibility of apparent diffusion coefficients measurements. J Magn Reson Imaging 59: 1170-1178, 2024.
24. Chen L, Shen F, Li Z, Lu H, Chen Y, Wang Z and Lu J: Diffusion-weighted imaging of rectal cancer on repeatability and cancer characterization: An effect of b-value distribution study. Cancer Imaging 18: 43, 2018.
25. Sumi M, Van Cauteren M, Sumi T, Obara M, Ichikawa Y and Nakamura T: Salivary gland tumors: Use of intravoxel incoherent motion MR imaging for assessment of diffusion and perfusion for the differentiation of benign from malignant tumors. Radiology 263: 770-777, 2012.
26. Palmucci S, Cappello G, Attinà G, Fuccio Sanzà G, Foti PV, Ettorre GC and Milone P: Diffusion-weighted MRI for the assessment of liver fibrosis: principles and applications. Biomed Res Int 2015: 874201, 2015.
27. Zhang G, Wang S, Wen D, Zhang J, Wei X, Ma W, Zhao W, Wang M, Wu G and Zhang J: Comparison of non-Gaussian and Gaussian diffusion models of diffusion weighted imaging of rectal cancer at 3.0 T MRI. Sci Rep 6: 38782, 2016.
28. Zhou M, Gong T, Chen M and Wang Y: High-resolution integrated dynamic shimming diffusion-weighted imaging (DWI) in the assessment of rectal cancer. Eur Radiol 33: 5769-5778, 2023.
29. Liu J, Li Q, Tang L, Huang Z and Lin Q: Correlations of mean and mimimum apparent diffusion coefficient values with the clinicopathological features in rectal cancer. Acad Radiol 28: S105-S111, 2021.
30. Du JF, Lu BL, Huang SY, Mao R, Zhang ZW, Cao QH, Chen ZH, Li SY, Qin QL, Sun CH, *et al*: A novel identification system combining diffusion kurtosis imaging with conventional magnetic resonance imaging to assess intestinal strictures in patients with Crohn's disease. Abdom Radiol (NY) 46: 936-947, 2021.
31. Manegold P, Taukert J, Neeff H, Fichtner-Feigl S and Thomusch O: The minimum distal resection margin in rectal cancer surgery and its impact on local recurrence–A retrospective cohort analysis. Int J Surg 70: 102, 2019.
32. Yan H, Wang PY, Wu YC and Liu YC: Is a distal resection margin of ≤1 cm safe in patients with intermediate- to low-lying rectal cancer? A systematic review and meta-analysis. J Gastrointest Surg 26: 1791-1803, 2022.